Original Article

MOLECULAR METABOLISM

The Peroxisome Proliferator-Activated Receptor α is dispensable for cold-induced adipose tissue browning in mice

Merel Defour [1], Wieneke Dijk [1], Philip Ruppert [1], Emmani B.M. Nascimento [2], Patrick Schrauwen [2], Sander Kersten [1,*]

ABSTRACT

Objective: Chronic cold exposure causes white adipose tissue (WAT) to adopt features of brown adipose tissue (BAT), a process known as browning. Previous studies have hinted at a possible role for the transcription factor Peroxisome Proliferator-Activated Receptor alpha (PPARα) in cold-induced browning. Here we aimed to investigate the importance of PPARα in driving transcriptional changes during cold-induced browning in mice.

Methods: Male wildtype and PPARα−/− mice were housed at thermoneutrality (28 °C) or cold (5 °C) for 10 days. Whole genome expression analysis was performed on inguinal WAT. In addition, other analyses were carried out. Whole genome expression data of livers of wildtype and PPARα−/− mice fasted for 24 h served as positive control for PPARα-dependent gene regulation.

Results: Cold exposure increased food intake and decreased weight of BAT and WAT to a similar extent in wildtype and PPARα−/− mice. Except for plasma non-esterified fatty acids, none of the cold-induced changes in plasma metabolites were dependent on PPARα genotype. Histological analysis of inguinal WAT showed clear browning upon cold exposure but did not reveal any morphological differences between wildtype and PPARα−/− mice. Transcriptomics analysis of inguinal WAT showed a marked effect of cold on overall gene expression, as revealed by principle component analysis and hierarchical clustering. However, wildtype and PPARα−/− mice clustered together, even after cold exposure, indicating a similar overall gene expression profile in the two genotypes. Pathway analysis revealed that cold upregulated pathways involved in energy usage, oxidative phosphorylation, and fatty acid β-oxidation to a similar extent in wildtype and PPARα−/− mice. Furthermore, cold-mediated induction of genes related to thermogenesis such as *Ucp1*, *Elovl3*, *Cox7a1*, *Cox8*, and *Cidea*, as well as many PPAR target genes, was similar in wildtype and PPARα−/− mice. Finally, pharmacological PPARα activation had a minimal effect on expression of cold-induced genes in murine WAT.

Conclusion: Cold-induced changes in gene expression in inguinal WAT are unaltered in mice lacking PPARα, indicating that PPARα is dispensable for cold-induced browning.

Keywords Cold; Adipose tissue browning; PPARα; Transcriptomics

1. INTRODUCTION

Cold exposure in mice causes specific white adipose tissue (WAT) depots to adopt features of brown adipose tissue (BAT), a process known as browning [1]. Browning is characterized by the appearance of adipocytes with multiple lipid droplets and by the acquisition of a thermogenic capacity, the latter of which is dependent on an increase in uncoupling protein (UCP) 1 [2]. Concurrent with the changes in cell morphology, the transcription of numerous genes involved in thermogenesis and lipid catabolism is strongly activated [3]. Recently, it was shown that human white adipose tissue is also capable of browning under condition of prolonged and severe adrenergic stress [4]. Nowadays, browning is considered as a potential molecular target to promote weight loss and improve metabolic risk factors, prompting investigation into the molecular mechanisms that drive browning.

One of the transcription factors that has been implicated in browning is PPARα [5]. PPARα is a member of the family of Peroxisome Proliferator-Activated Receptors, which play key roles in the regulation of lipid homeostasis and oxidative metabolism [6–8]. Three different PPAR subtypes exist in mammals: PPARα, PPARδ (also referred to as PPARβ), and PPARγ, each with a distinct tissue expression profile and set of functions. PPARs regulate gene expression in response to binding small lipophilic ligands and function as a heterodimeric complex with the retinoid X receptor RXR [9–11]. The ligands for PPARs include a variety of synthetic and endogenous compounds

[1]Nutrition, Metabolism and Genomics Group, Division of Human Nutrition and Health, Wageningen University, Stippeneng 4, 6708 WE Wageningen, The Netherlands [2]Department of Human Biology and Human Movement Sciences, NUTRIM School for Nutrition and Translational Research in Metabolism, Maastricht University Medical Center, PO Box 616, 6200 MD Maastricht, The Netherlands

*Corresponding author. E-mail: sander.kersten@wur.nl (S. Kersten).

Received January 8, 2018 • Revision received January 25, 2018 • Accepted January 31, 2018 • Available online 9 February 2018

https://doi.org/10.1016/j.molmet.2018.01.023

ranging from industrial chemicals to specific drug classes, fatty acids, eicosanoids, and other lipid species [12].

The PPARα subtype is expressed in several tissues, with the highest expression levels in mice found in brown adipose tissue (BAT) and liver, followed by kidney, heart, skeletal muscle and intestine [13,14]. At the physiological level, PPARα is mainly known as the master regulator of lipid metabolism in the liver during fasting. This notion is based on the finding that fasted whole-body or liver-specific PPARα−/− mice have a severe metabolic phenotype characterized by hypoglycemia, hypoketonemia, elevated plasma non-esterified fatty acids (NEFAs), and a fatty liver [15–17]. These metabolic defects are rooted in reduced expression of hundreds of genes involved in numerous metabolic pathways covering nearly every aspect of hepatic lipid metabolism [18].

The PPARγ subtype is predominantly expressed in colonocytes, macrophages, and adipocytes [13]. It is mainly known as the target for the insulin-sensitizing thiazolidinedione drugs [19]. In addition, PPARγ is essential for the differentiation of brown and white adipocytes [20]. In mice, loss of PPARγ fails to yield viable offspring [21], while in humans homozygosity for loss-of-function mutations in PPARγ leads to a form of lipodystrophy [22].

Both PPARα and PPARγ have been implicated in browning [5]. With respect to PPARγ, treatment of mice with synthetic PPARγ agonists promotes adipose tissue browning, as shown by the appearance of multilocular adipocytes and the increased expression of thermogenic genes such as *Ucp1*, triggering thermogenic capacity in WAT [23–25]. Conversely, mice carrying a functionally impaired mutant form of PPARγ have reduced adipose tissue browning and an impaired thermogenic capacity after treatment with the β3-adrenergic agonist CL316,243 [26]. Furthermore, activation of PPARγ in human preadipocytes and adipocytes increased expression of *UCP1* and other browning-related genes [27,28].

The role of PPARα in browning is less clear. Although a number of studies have implicated PPARα in CL316,243-induced browning [27,29], no studies have carefully examined the transcriptional role of PPARα during cold-induced browning. Based on the reported attenuation of browning by PPARα ablation after CL316,243 treatment [27,29], and considering the marked induction of PPARα mRNA and protein during cold-induced browning [30,31], we hypothesized that PPARα is essential for stimulating gene expression in inguinal WAT in response to cold. The objective of this study was to verify this hypothesis and investigate the importance of PPARα in cold-induced browning in mice.

2. METHODS

2.1. Animals and diet

Male and female wildtype and PPARα−/− mice that had been backcrossed on a pure C57Bl/6J background for more than 10 generations were acquired from Jackson Laboratories (no. 000664 and 008154, respectively). The mice were further bred at the animal facility of Wageningen University under specific pathogen free conditions to generate the number of mice necessary for the experiments. For the chronic cold experiment, 40 three-to four-month-old male wildtype and PPARα−/− mice were placed at thermo-neutral temperature (28 °C) for 5 weeks. Thereafter, 20 wildtype and 20 PPARα−/− mice were randomly distributed across 2 groups: half of the mice of each genotype were kept at thermo-neutral temperature and half of the mice of each genotype was placed at 21 °C for one week followed by a period of 10 days in the cold (5 °C) (n = 10 per group). For cold exposure, mouse cages were placed in a cold cabinet that was kept at 5 °C (ELDG800, VDW Coolsystems, Geldermalsen). Mice had ad libitum access to chow feed and water. Body weight and body temperature were monitored daily during the cold exposure period. Body temperature of the cold-exposed mice was monitored via read-out of transponders (IPTT-300) that were injected subcutaneously prior to the experiment (Bio Medic Data Systems, Seaford, USA). For the acute cold experiment, three-to four-month-old male wildtype and PPARα−/− mice were placed at thermo-neutral temperature (28 °C) for 5 weeks. Thereafter, the mice were placed in the cold (5 °C) for 24 h (n = 10 per group). For the fasting experiment, three-to four-month-old male wildtype and PPARα−/− mice were either fasted for 24 h or had food available ad libitum (n = 10–11 per group). For PPAR agonist treatment, Sv129 male mice were placed on a high fat diet (formula D12451 Research Diets, Inc., manufactured by Research Diet Services, Wijk bij Duurstede) for 21 weeks with the addition of Wy14,643 (0.1% w/w of feed) or rosiglitazone (0.01% w/w of feed) during the last week. All mice were housed at the animal facility of Wageningen University. Mice were housed in individual cages with normal bedding and cage enrichment on a 12 h light–dark cycle. They had visual and auditory contact with littermates. At the end of the study, between 9.00h and 11.00h, blood was collected via orbital puncture under isoflurane anesthesia into EDTA tubes. Mice were euthanized via cervical dislocation, after which tissues were excised and directly frozen in liquid nitrogen or prepared for histology. All studies were approved by the Animal Ethics Committee of Wageningen University and by the Central Animal Testing Committee (CCD, AVD104002015236).

2.2. RNA isolation and quantitative PCR

Total RNA was extracted from cells using TRIzol reagent (Life Technologies, Bleiswijk, The Netherlands). For tissues, total RNA was isolated using the RNeasy Micro kit from Qiagen (Venlo, The Netherlands). Subsequently, 500 ng RNA was used to synthesize cDNA using iScript cDNA synthesis kit (Bio-Rad Laboratories, Veenendaal, The Netherlands). Messenger RNA levels of selected genes were determined by reverse transcription quantitative PCR using SensiMix (Bioline; GC Biotech, Alphen aan den Rijn, The Netherlands) on a CFX384 real-time PCR detection system (Bio-Rad Laboratories, Veenendaal, the Netherlands). The housekeeping gene *36b4* was used for normalization.

2.3. Histology/immunohistochemistry

Fresh WAT tissues were fixed in 4% paraformaldehyde, dehydrated, and embedded in paraffin. Hematoxilin & Eosin staining was performed using standard protocols.

2.4. Plasma measurements

Plasma concentrations of glucose (Sopachem, Ochten, the Netherlands), triglycerides, cholesterol, ketone bodies (Instruchemie, Delfzijl, the Netherlands), glycerol (Sigma–Aldrich, Houten, the Netherlands), and non-esterified fatty acids (Wako Chemicals, Neuss, Germany; HR(2) Kit) were determined following the manufacturers' instructions.

2.5. Liver triglycerides

Liver triglyceride levels were determined in 10% liver homogenates prepared in buffer containing Sucrose 250 mM, EDTA 1 mM, Tris–HCl 10 mM pH 7.5 using a commercially available kit from Instruchemie (Delfzijl, The Netherlands).

2.6. Microarray analysis

Microarray analysis was performed on inguinal adipose tissue samples from 5 to 6 mice of each group and liver samples from 5 mice per group. RNA was isolated as described above and subsequently purified using

the RNeasy Micro kit from Qiagen (Venlo, The Netherlands). RNA integrity was verified with RNA 6000 Nano chips on an Agilent 2100 bioanalyzer (Agilent Technologies, Amsterdam, The Netherlands). Purified RNA (100 ng) was labeled with the Ambion WT expression kit (Carlsbad, CA) and hybridized to an Affymetrix Mouse Gene 1.1 ST array plate (Affymetrix, Santa Clara, CA). Hybridization, washing, and scanning were carried out on an Affymetrix GeneTitan platform according to the manufacturer's instructions. Normalized expression estimates were obtained from the raw intensity values applying the robust multi-array analysis preprocessing algorithm available in the Bioconductor library AffyPLM with default settings [32,33]. Probe sets were defined according to Dai et al. [34]. In this method probes are assigned to Entrez IDs as a unique gene identifier. In this study, probes were reorganized based on the Entrez Gene database, build 37, version 1 (remapped CDF v22). The microarray dataset was filtered by only including probe sets with expression values higher than 20 on at least 4 arrays. In addition, an Inter Quartile Range (IQR) cut-off of 0.25 was used to filter out genes that showed no variation between the conditions, leaving a total of 8174 genes for further statistical analysis. The P values were calculated using an Intensity-Based Moderated T-statistic (IBMT) [35]. Genes were defined as significantly changed when $P < 0.001$.

Gene set enrichment analysis (GSEA) was used to identify gene sets that were enriched among the upregulated or downregulated genes [36]. Genes were ranked based on the IBMT-statistic and subsequently analyzed for over- or underrepresentation in predefined gene sets derived from Gene Ontology, KEGG, National Cancer Institute, PFAM, Biocarta, Reactome and WikiPathways pathway databases. Only gene sets consisting of more than 15 and fewer than 500 genes were taken into account. Statistical significance of GSEA results was determined using 1,000 permutations.

As an alternative strategy to identify pathways up- or down-regulated by cold or fasting, Ingenuity Pathway Analysis (Ingenuity Systems, Redwood City, CA) was performed. Input criteria were a relative fold change equal to or above 1.5 and an IBMT P-value$<$0.001. Array data have been submitted to the Gene Expression Omnibus (GSE110420). The microarray analysis on livers of fed and fasted wildtype and PPAR$\alpha$$-/-$ mice was previously published (GSE17863) [37], as was the microarray analysis on WAT of PPAR agonist treated mice (GSE11295) [38].

2.7. Isolation and differentiation of primary adipocytes

WAT was dissected from wild-type and PPAR$\alpha$$-/-$ mice and put in DMEM supplemented with 1% Pen/Strep and 1% BSA. Tissues of 3 mice were pooled, minced with scissors, and digested for 1 h at 37 °C in collagenase-containing medium (DMEM with 3.2 mM $CaCl_2$, 1.5 mg/ml collagenase type II (Sigma–Aldrich), 10% FBS, 0.5% BSA (Sigma-Aldrich) and 15 mM HEPES). After digestion, the cell mixture was passed over a 100 μm cell strainer and centrifuged at 1600 rpm for 10 min. Supernatant was removed and the pellet containing the stromal vascular fraction was re-suspended in erythrocyte lysis buffer (155 mM NH_4Cl, 12 mM $NaHCO_3$, 0.1 mM EDTA) and incubated for 2–3 min at room temperature. Following neutralization, cells were centrifuged at 1200 rpm for 5 min. Cells were re-suspended in DMEM containing 10% FBS and 1% Pen/Strep and plated. Upon confluence, cells were differentiated following standard protocol of 3T3-L1 cells, as described previously [39].

2.8. Isolation and differentiation of human primary adipocytes derived from WAT

The isolation and differentiation of adipocytes derived from human WAT has been described before [40]. In short, the stromal vascular fraction was obtained from subcutaneous WAT during thyroid surgery using a collagenase digestion.

Differentiation was initiated for 7 days with differentiation medium containing biotin (33 μM), pantothenate (17 μM), insulin (100 nM), dexamethasone (100 nM), IBMX (250 μM), rosiglitazone (5 μM), T3 (2 nM), and transferrin (10 μg/ml). Cells were transferred to maintenance medium consisting of biotin (33 μM), pantothenate (17 μM), insulin (100 nM), dexamethasone (10 nM), T3 (2 nM), and transferrin (10 μg/ml) for another 5 days in the presence of absence of 300 nM GW7647.

The study was reviewed and approved by the ethics committee of Maastricht University Medical Center (METC 10-3-012, NL31367.068.10). Informed consent was obtained before surgery, and participants did not receive a stipend.

2.9. Oxygen consumption in differentiated adipocytes derived from human BAT

Differentiated adipocytes were incubated for 1 h at 37 °C in unbuffered XF assay medium supplemented with 2 mM GlutaMAX, 1 mM sodium pyruvate, and 25 mM glucose. To determine NE-stimulated mitochondrial uncoupling, oxygen consumption was measured using bioanalyzer from Seahorse Bioscience after addition of 2 μM oligomycin, which inhibited ATPase, followed by 1 μM NE. Maximal respiration was determined following 0.3 μM FCCP-induced determined. 1 μM antimycin A and rotenone was added to correct for non-mitochondrial respiration.

2.10. Statistical analysis

Data are presented as mean ± SEM. Comparisons between two groups were made using two-tailed Student's t-test. $P < 0.05$ was considered as statistically significant. Excel software (version 2016) was used for statistical analysis.

3. RESULTS

3.1. PPARα and PPARα target genes are upregulated during cold-induced browning

Quantitative PCR indicated that *Ppara* mRNA levels were markedly increased in inguinal WAT but not gonadal WAT after 10 days of cold exposure as compared to thermoneutrality (Figure 1A), suggesting a role of PPARα in cold-induced browning in mice. The mRNA expression level of *Ppara* in inguinal WAT after cold approaches the robust expression level of *Ppara* in brown fat (Figure 1B). Analysis of an existing microarray dataset (GSE51080) indicated that *Ppara* is among the most highly induced genes in murine inguinal adipose tissue in response to cold (Figure 1C) [41]. Along with *Ppara* and genes associated with browning such as *Ucp1*, *Cidea*, and *Elovl3*, many target genes of PPARα were highly induced by cold in inguinal WAT, including *Pank1*, *Slc25a20*, *Pdk4*, *Fbp2*, *Plin5, Acadl* and *Acaa2* (Figure 1C). A large similarity was observed between the inductions in gene expression elicited by cold in inguinal adipose tissue and the gene expression changes caused by PPARα activation in the liver using a synthetic PPARα agonist (Figure 1C), again suggesting activation of PPARα in inguinal WAT during cold. Similar results were obtained using another microarray dataset on the effect of cold in murine inguinal WAT (GSE13432, Supplemental Figure 1) [42]. According to gene set enrichment analysis, PPARα target genes were also highly enriched among the cold-induced genes (Figure 1D). Together, these data suggest a possible role for PPARα in cold-induced browning.

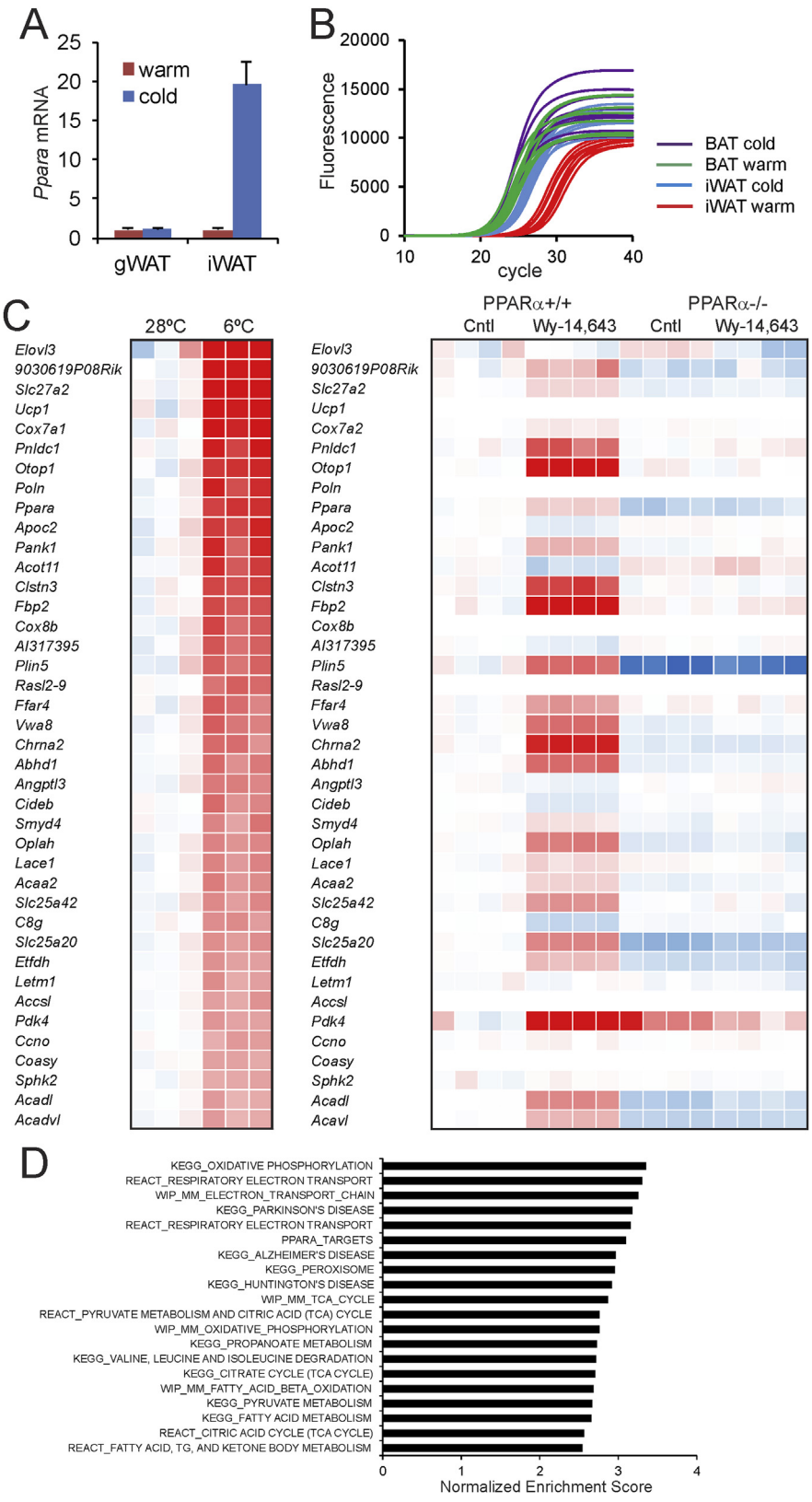

Figure 1: PPARα is highly upregulated during cold-induced browning. (A) Relative gene expression of PPARα in gonadal WAT and inguinal WAT of wildtype mice after 10 days at 28 °C (warm, n = 6–8) or 5 °C (cold, n = 10) [51]. Data are presented as mean ± SEM. (B) Quantitative PCR amplification curves of *Ppara* in inguinal WAT and BAT of wildtype mice exposed to cold (5 °C) or thermoneutrality (28 °C, warm) for 10 days. (C) Heatmap of the top 40 most highly induced genes in subcutaneous adipose tissue of mice after 10 days at 6 °C as compared to 10 days at 28 °C (GSE51080). In parallel, the expression profiles are shown of the same genes in livers of wild type and PPARα−/− mice treated with Wy-14.643 for 5 days (GSE8295). (D) Top 20 gene sets induced by cold-exposure in subcutaneous adipose tissue of mice after 7 days at 4 °C as compared to 7 days a 30 °C (GSE13432), determined by gene set enrichment analysis. Gene sets were ranked according to normalized enrichment score.

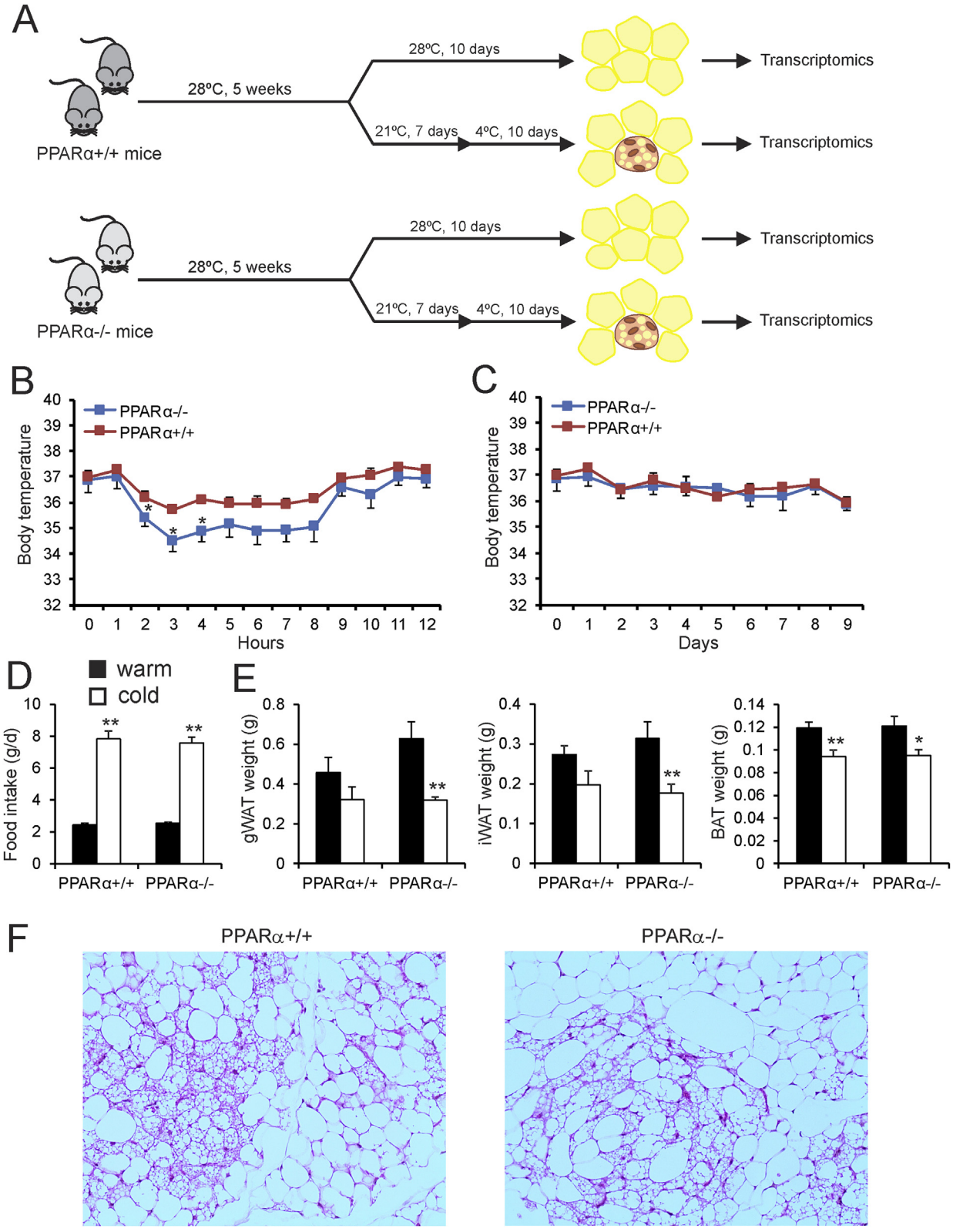

Figure 2: Transient hypothermia in PPARα−/− mice exposed to cold. (A) Schematic representation of the cold intervention in wildtype and PPARα−/− mice. (B–C) Body temperature during the first 12 h of cold exposure and assessed daily during the full 10 days of cold exposure. Asterisk indicates significantly different from wildtype mice according to Student's t-test ($P < 0.05$). (D) Feed intake after 9 days of exposure to cold (5 °C, cold) or thermoneutrality (28 °C, warm). (E) Adipose tissue weights of gonadal WAT, inguinal WAT, and BAT of wild type and PPARα−/− mice exposed to cold (5 °C) or thermoneutrality (28 °C) for 10 days. N = 10 per group. Asterisk indicates significantly different from thermoneutral mice according to Student's t-test (*$P < 0.05$, **$P < 0.01$). (F) Representative Hematoxilin and eosin staining of inguinal WAT of cold-exposed wildtype and PPARα−/− mice. Inguinal WAT shows large variability in the degree of browning. Sections of inguinal WAT that show very significant browning were selected. Images are at 100× magnification.

3.2. Cold-induced changes in WAT morphology are unaltered in PPARα−/− mice

To investigate the role of PPARα in cold-induced browning, male wildtype and PPARα−/− mice were studied after 10 days of cold exposure (5 °C) (Figure 2A). For comparison, another group of wildtype and PPARα−/− were studied after a prolonged stay at thermoneutrality (28 °C). Cold exposure caused a transient decrease in body temperature, which was significantly more pronounced in the PPARα−/− mice than in the wildtype mice (Figure 2B). The difference in body temperature disappeared after prolonged cold exposure (Figure 2C). As expected, cold exposure markedly increased food intake (Figure 2D). However, no differences in food intake were observed between wildtype and PPARα−/− mice (Figure 2D). Also, no differences in the weight of the inguinal WAT, gonadal WAT, and interscapular BAT depots were observed between wildtype and PPARα−/− mice, neither in the thermoneutral nor in the cold-exposed mice (Figure 2E). To examine any potential morphological differences in the inguinal WAT of wildtype and PPARα−/− mice, we performed H&E staining (Figure 2F). The inguinal WAT of both sets of mice showed the characteristic features of browning, as revealed by the presence of numerous multilocular brown fat-like cells. However, no obvious differences could be observed in the degree of browning between the wildtype and PPARα−/− mice (Figure 2F).

Next, we measured the levels of various metabolites in the blood plasma. In the cold-exposed mice, levels of non-esterified fatty acids and cholesterol were significantly higher in plasma of PPARα−/− mice compared to wildtype mice, a finding which was not observed under thermoneutral conditions (Figure 3). By contrast, plasma levels of triglycerides, glycerol, ketones, and glucose were not significantly different between cold-exposed PPARα−/− and wildtype mice. These data indicate that the absence of PPARα leads to a modest metabolic phenotype in cold-exposed mice.

3.3. Cold induces similar changes in gene expression in wildtype and PPARα−/− mice at the whole genome level

To gain insight into the role of PPARα in cold-induced browning, we performed whole genome expression profiling on the inguinal WAT depot of wildtype and PPARα−/− mice exposed to thermoneutrality or cold. As a strong positive reference for PPARα-dependent gene regulation, a parallel whole genome expression analysis was performed on the livers of wildtype and PPARα−/− mice subjected to fasting for 24 h or fed ad libitum.

Volcano plot analysis indicated that the differences in gene expression in inguinal WAT between cold-exposed wildtype and PPARα−/− mice are very modest (Figure 4A), certainly when compared with the differences in liver gene expression between wildtype and PPARα−/− mice after fasting (Figure 4B). Indeed, after cold, expression of only 50 genes was significantly lower and expression of 20 genes was significantly higher in inguinal WAT of PPARα−/− mice as compared to wildtype mice ($P < 0.001$, fold-change>1.2) (Figure 4C). By comparison, after fasting, expression of 1224 genes was significantly lower and expression of 1328 genes was significantly higher in the liver of PPARα−/− mice as compared to wildtype mice ($P < 0.001$, fold-change>1.2) (Figure 4C). Principle component analysis and hierarchical clustering clearly separated the inguinal WAT samples of the cold-exposed mice and the thermoneutral mice, illustrating the pronounced impact of cold on overall gene expression in inguinal WAT (Figure 5A). However, within the cold and thermoneutral groups, wildtype and PPARα−/− mice did not separate into distinct clusters, suggesting a minimal effect of PPARα deletion on overall gene regulation in cold-exposed inguinal WAT. By contrast, principle component analysis and hierarchical clustering markedly separated the livers of fasted wildtype and PPARα−/− mice (Figure 5B).

Scatter plot analysis confirmed that the effect of cold on overall gene expression in inguinal WAT is nearly identical in wildtype and

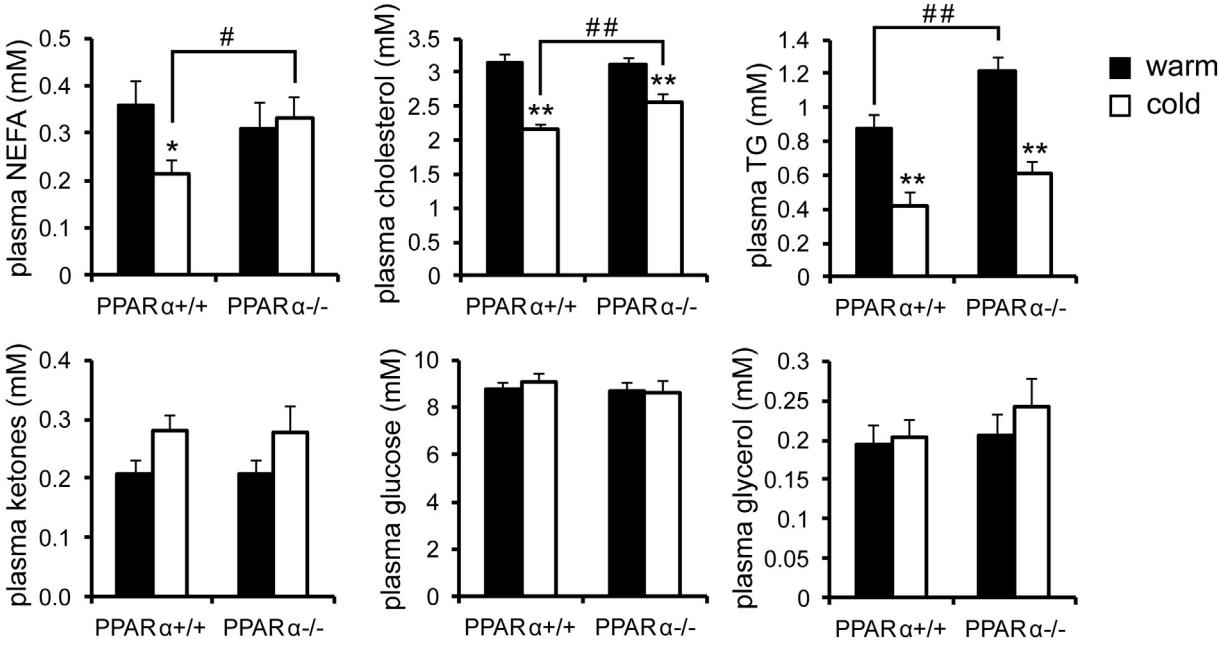

Figure 3: Cold does not amplify differences in plasma metabolites between wildtype and PPARα−/− mice. Plasma metabolite concentrations in wildtype and PPARα−/− mice exposed to cold (5 °C) or thermoneutrality (28 °C) for 10 days. Asterisk indicates significantly different from thermoneutral mice according to Student's t-test (*$P < 0.05$, **$P < 0.01$). Pound sign indicates significant difference between wildtype and PPARα−/− mice according to Student's t-test (#$P < 0.05$, ##$P < 0.01$). N = 10 per group.

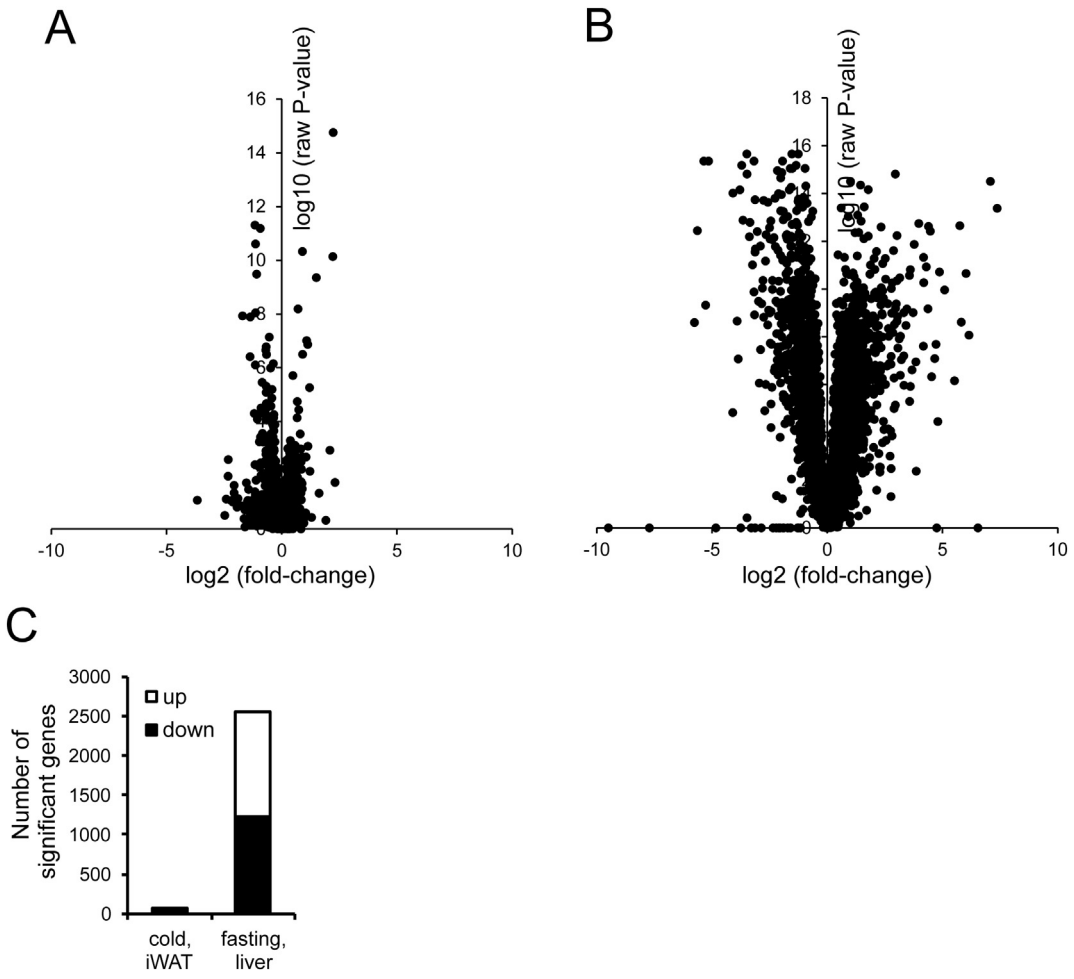

Figure 4: Comparative analysis of the effect of cold and fasting in wildtype and PPARα−/− mice. A) Volcano plot in which ^{2}log(fold-change) is plotted against $-^{10}$log-(P-value) for comparison between inguinal WAT of wildtype and PPARα−/− mice after 10-day cold exposure (B) Volcano plot in which ^{2}log(fold-change) is plotted against $-^{10}$log-(P-value) for comparison between liver of wildtype and PPARα−/− mice after 24 h fasting. (C) Number of genes in inguinal WAT that are significantly different between wildtype and PPARα−/− mice after 10-day cold exposure, and the number of genes in liver that are significantly different between wildtype and PPARα−/− mice after 24 h fasting. The number of differentially expressed genes was calculated based on a statistical significance cut-off of $P < 0.001$ (IBMT regularized paired t-test) and fold-change >1.2. Genes were separated according to up- or down-regulation.

PPARα−/− mice (Figure 5C). Also, the cold-induced changes in gene expression of several classical PPARα target genes was virtually identical in inguinal WAT of wildtype and PPARα−/− mice (Figure 5C, red dots). By contrast, the effect of fasting on overall gene expression in liver was very distinct between wildtype and PPARα−/− mice, illustrating the importance of PPARα in hepatic gene regulation during fasting (Figure 5D). These data indicate that at the whole genome level, inguinal WAT of PPARα−/− mice cannot be distinguished from inguinal WAT of wildtype mice, both at thermoneutral and cold conditions. In contrast, livers of PPARα−/− mice can easily be distinguished from wildtype mice, in particular after fasting.

3.4. Cold-sensitive pathways are similarly induced in inguinal WAT in wildtype and PPARα−/− mice

To further evaluate the browning effect in wildtype and PPARα−/− mice, we compared the effect of cold on biological pathways in the two sets of mice using Ingenuity Pathway Analysis and Gene Set Enrichment Analysis. The most significant cold-induced pathways in the wildtype mice were mainly related to the electron transport chain and oxidative phosphorylation (Figure 6A). Consistent with the data presented above—showing a lack of difference in cold-induced expression changes between wildtype and PPARα−/− mice—the enrichments scores for the cold-induced pathways were nearly identical in the wildtype mice and PPARα−/− mice (Figure 6A). Similarly, according to Ingenuity Pathway Analysis, the most significant cold-induced pathways in inguinal WAT were related to oxidative phosphorylation, the tricarboxylic acid cycle, fatty acid oxidation, and other catabolic pathways, and had very similar significance scores in wildtype and PPARα−/− (Figure 6B). Remarkably, the pathway named PPARA targets was equally induced by cold in wildtype and PPARα−/− mice, indicating that PPARα is dispensable for regulation of PPARα targets by cold in inguinal WAT. By contrast, the results of Gene Set Enrichment Analysis and Ingenuity Pathway Analysis for the fasting-induced changes in hepatic gene expression were very distinct in the wildtype mice and PPARα−/− mice. Specifically, enrichment scores and significance scores for many pathways related to PPAR signaling and fatty acid catabolism were very high in the wildtype mice yet were much lower or even opposite in the PPARα−/− mice

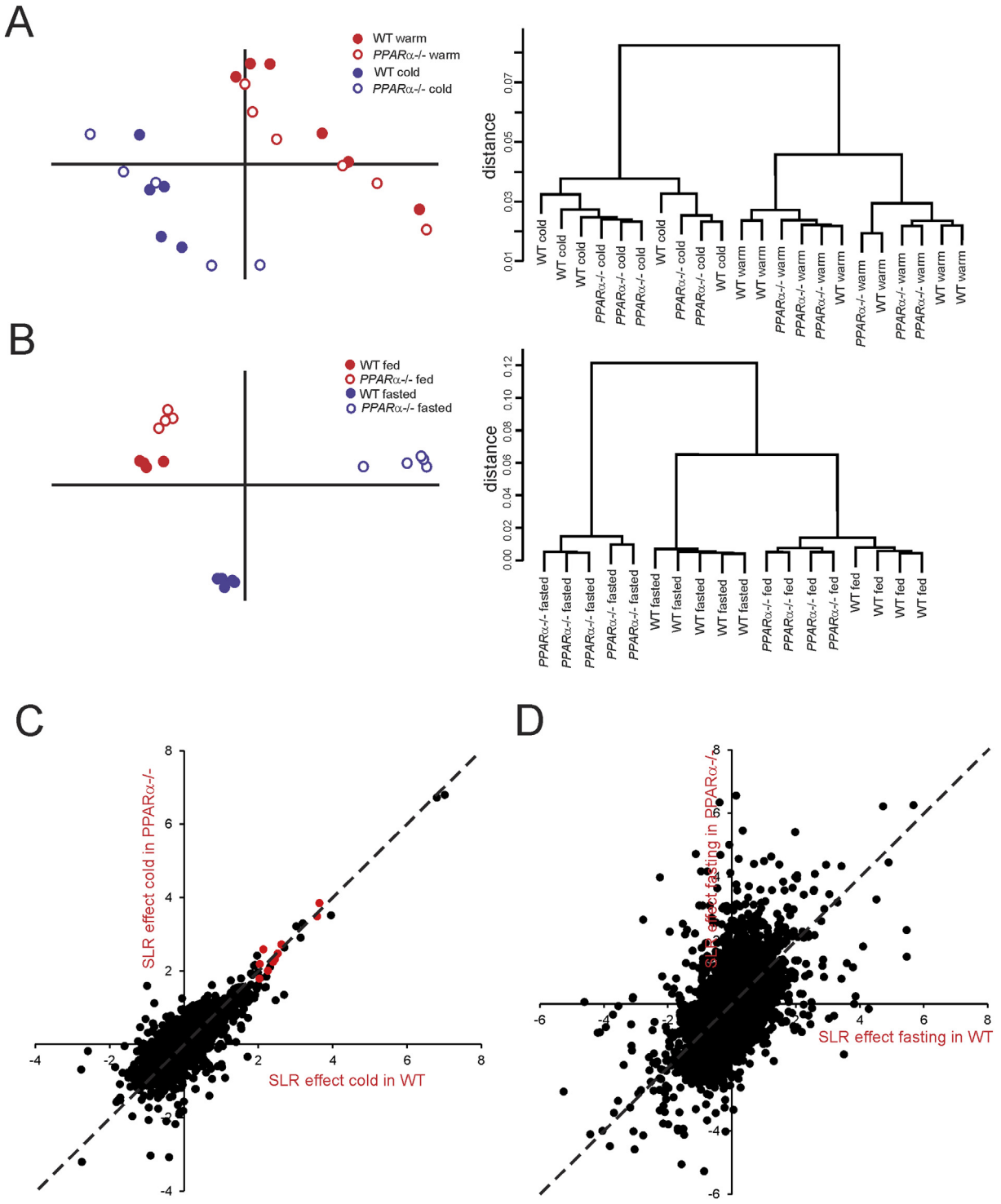

Figure 5: Distinct clustering of inguinal WAT of thermoneutral and cold-exposed wildtype and PPARα−/− mice. (A) Left panel: Principle component analysis of transcriptomics data from inguinal WAT of the thermoneutral and cold-exposed wildtype and PPARα−/− mice. The graph shows the clear separation of mice according to treatment, while the two genotypes are mixed. Right panel: Hierarchical clustering of transcriptomics data from the thermoneutral and cold-exposed wildtype and PPARα−/− mice. The dendogram reveals the distinct clustering and separation based on treatment, but not based on genotype. (B) Left panel: Principle component analysis of transcriptomics data from livers of fed and fasted wildtype and PPARα−/− mice. The graph shows the clear separation between the genotypes in both fed and fasted state. Right panel: Hierarchical clustering of transcriptomics data from the fed and fasted wildtype and PPARα−/− mice. The dendogram reveals the distinct clustering and separation according to treatment and genotypes. (C) Correlation plot showing gene expression changes in response to cold in wildtype (x-axis) versus PPARα−/− mice (y-axis) (expressed as signal log ratio). Well established PPARα target genes are highlighted in red (*Cox7a1*, *Slc27a2*, *Cidea*, *Gys2*, *Pank1*, *Gyk*, *Plin5*, *Pdk4*, *Slc25a20*, *Hadhb*). (D) Correlation plot showing gene expression changes in response to fasting in wildtype (x-axis) versus PPARα−/− mice (y-axis) (expressed as signal log ratio).

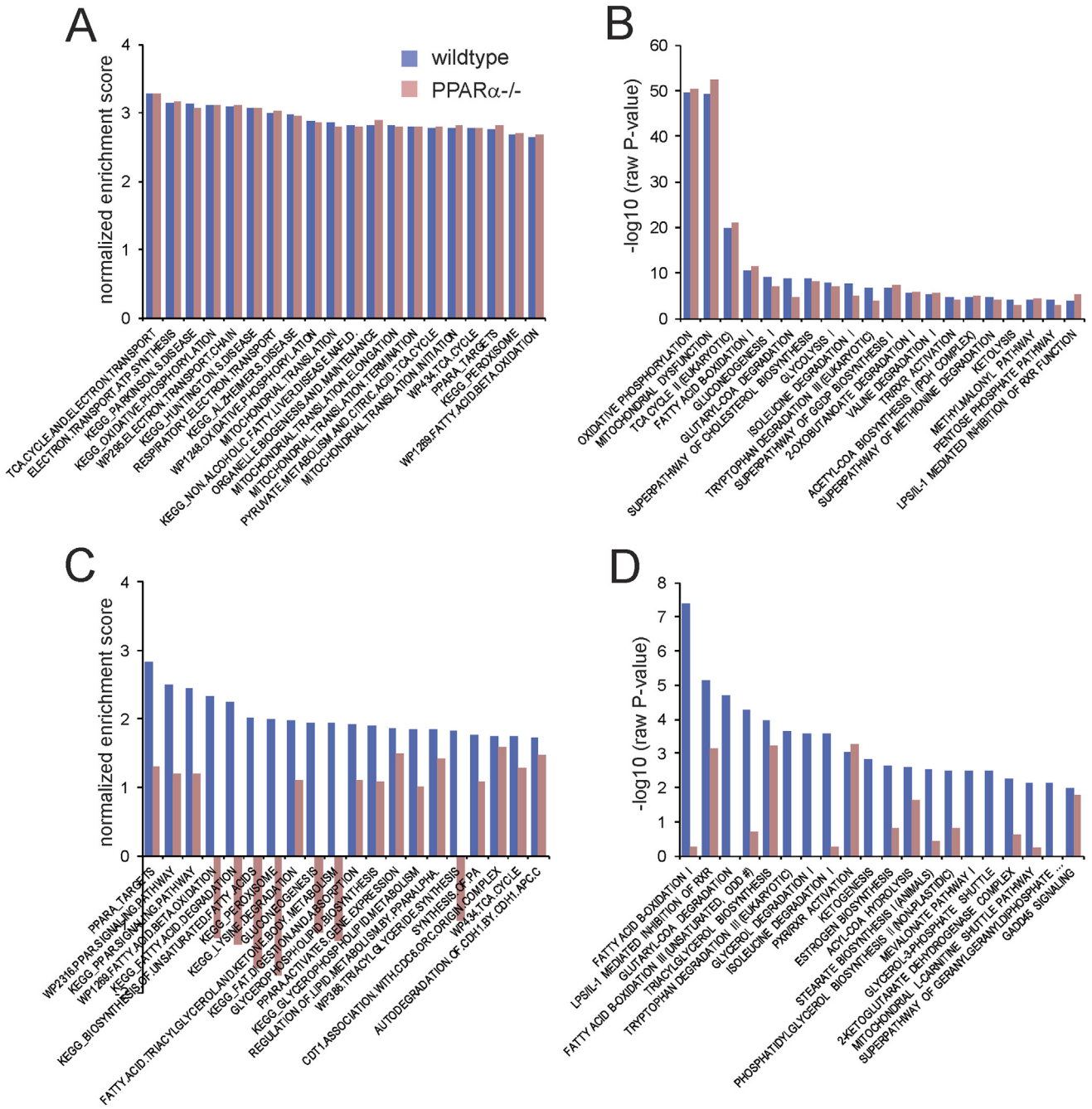

Figure 6: Minimal effect of PPARα deletion in inguinal WAT at the pathway level. A) Gene set enrichment analysis of the effect of 10-day cold exposure in inguinal WAT of wildtype (blue bars) and PPARα−/− mice (red bars). The top 20 gene sets with the highest normalized enrichment scores in wildtype mice are shown. B) Ingenuity pathway analysis (Biological Pathways) of the effect of 10-day cold exposure in inguinal WAT of wildtype (blue bars) and PPARα−/− mice (red bars). The top 20 most significant pathways in the wildtype mice are shown. C) Gene set enrichment analysis of the effect of 24h fasting in liver of wildtype (blue bars) and PPARα−/− mice (red bars). The top 20 gene sets with the highest normalized enrichment scores in wildtype mice are shown. D) Ingenuity pathway analysis (Biological Pathways) of the effect of fasting in liver of wildtype (blue bars) and PPARα−/− mice (red bars). The top 20 most significant pathways in the wildtype mice are shown.

(Figure 6C,D). Taken together, these data show that at the pathway level, the absence of PPARα does not have a noticeable influence on the induction of metabolic pathways by cold in inguinal WAT.

3.5. Cold-sensitive genes are similarly induced in inguinal WAT in wildtype and PPARα−/− mice

To further zoom in at the level of individual genes, we selected the top 50 of most highly induced genes by cold exposure in inguinal WAT in the wildtype mice, ranked according to fold-change (Figure 7A). As expected, the most highly induced gene by cold was *Ucp1*, followed by other well-known cold-induced genes such as *Elovl3*, *Cox7a1*, and *Cidea*. This top 50 list also includes many well-established PPARα target genes in the liver, including *Gyk*, *Gys2*, *Plin5*, *Pdk4*, *Hadhb*, *Slc25a20*, *Gpd2*, and *Acadvl*, as well as *Ppara* itself (Figure 7A). Consistent with the data presented above, the cold-induced changes in gene expression were generally similar in the PPARα−/− mice. Out of the 641 genes that were induced by cold (fold-change>1.5, $P < 0.001$), only 5 genes had a significantly lower expression in the cold-exposed PPARα−/− mice than in the cold-exposed wildtype mice (fold-change <−1.5, $P < 0.001$). These genes include

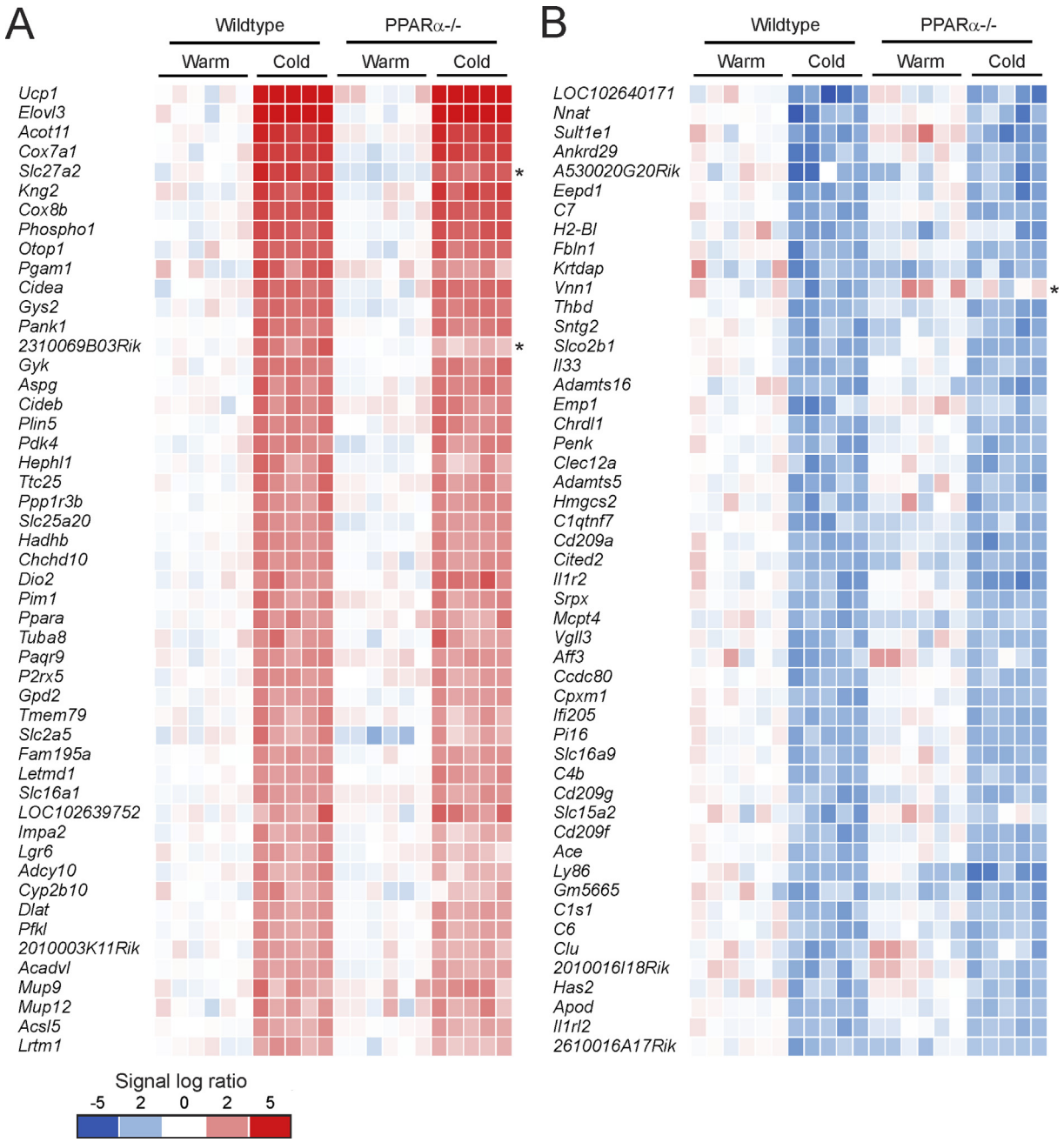

Figure 7: Cold induces parallel changes in gene expression in wildtype and PPARα−/− mice. A) Comparative gene expression analysis in inguinal WAT of thermoneutral and cold-exposed wildtype and PPARα−/− mice, showing the top 50 most highly induced genes by cold in wildtype mice ($P < 0.001$, ranked according to fold-change). B) Comparative gene expression analysis in inguinal WAT of thermoneutral and cold-exposed wildtype and PPARα−/− mice, showing the top 50 most highly repressed genes by cold in wildtype mice ($P < 0.001$, ranked according to fold-change). Genes marked with asterisk were significantly different between and cold-exposed wildtype and PPARα−/− mice ($P < 0.001$).

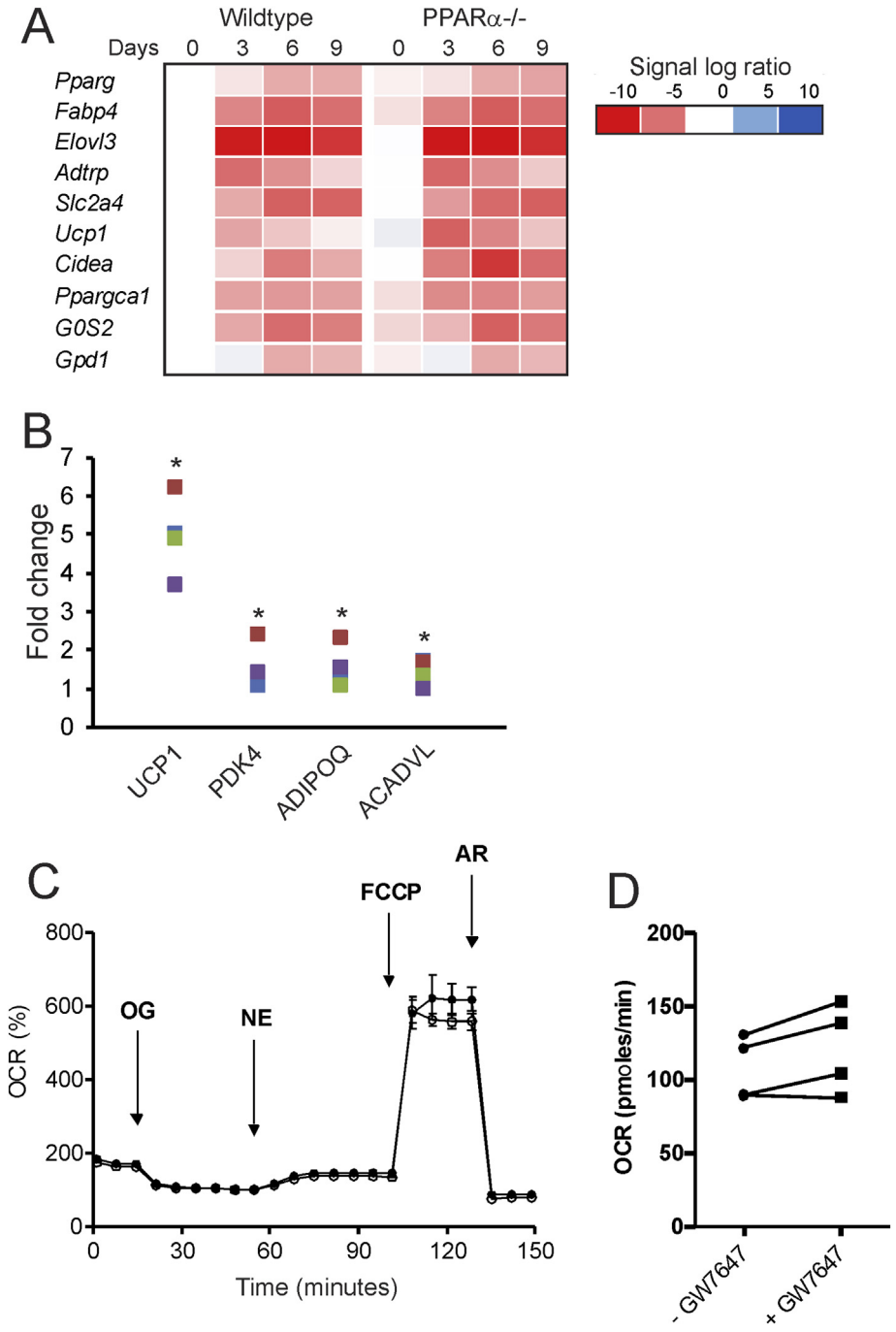

Figure 8: Role of PPARα in *in vitro* browning. (A) Stromal vascular cells of wildtype and PPARα−/− mice were differentiated towards brown-like adipocytes. Relative gene expression of adipogenic markers and brown adipocyte markers as determined by qPCR and expressed in a heatmap. (B) Differentiating human pre-adipocytes derived from subcutaneous WAT were treated with GW7647 (300 nM) for 5 days. Relative gene expression of *UCP1*, *PDK4*, *ADIPOQ*, and *ACADVL* in differentiated adipocytes is shown. The different colors represent the primary adipocytes from 4 different individuals. For each individual, the expression level of the untreated adipocytes was set at 1. (C) Cellular respiration trace measured in adipocytes derived from human WAT on bioanalyzer from Seahorse with GW7647 (open circles) or without GW7647 (closed circles). (D) Basal cellular respiration in adipocytes derived from human WAT with or without GW7647 treatment during differentiation.

2310069B03Rik, *Adprhl1*, and the established PPARα targets *Slc27a2*, *Fbp2*, and *Ehhad* [18]. A similar picture was observed for genes that were downregulated by cold (Figure 7B). Indeed, downregulation of gene expression by cold was generally unaffected in the PPARα−/− mice. Out of the 420 genes that were downregulated by cold (fold-change <-1.5, $P < 0.001$), only 2 genes had a significantly higher expression in the cold-exposed PPARα−/− mice than in the exposed wildtype mice (fold-change>1.5, $P < 0.001$), which were *Vnn1* and *Sema5a*. These data suggest that except for a very limited number of genes, mostly representing direct PPARα target genes, the changes in gene expression in inguinal WAT induced by cold were nearly identical in wildtype and PPARα−/− mice.

3.6. Role of PPARα in *in vitro* browning

Next, to examine the potential role of PPARα in *in vitro* browning, we first studied the differentiation of wildtype and PPARα−/− stromal vascular cells from inguinal WAT. Adipocyte differentiation was accompanied by the marked induction of classical adipogenic markers, including *Pparg*, *Fabp4*, *Slc2a4*, and *Gpd1*, as well as induction of brown adipocyte markers, such as *Ppargc1a*, *Cidea*, *Elovl3*, and *Ucp1* (Figure 8A). Intriguingly, whereas induction of classical adipogenic markers was not different between wildtype and PPARα−/− adipocytes, expression of brown adipocyte markers was elevated in PPARα−/− compared to wildtype adipocytes (Figure 8A). These data do not support the notion that PPARα is required for the activation of the genes underlying browning.

To investigate the ability of PPARα to activate *in vitro* browning in human adipocytes, we treated human primary adipocytes obtained from subcutaneous adipose tissue with the synthetic PPARα agonist GW7647. Consistent with previous data, GW7647 increased *UCP1* mRNA levels (Figure 8B) [27]. In addition, GW7647 modestly upregulated the expression of *PDK4*, *ADIPOQ*, and *ACADVL* (Figure 8B). Despite the approximately 5-fold increase in *UCP1* mRNA, no effect of GW7647 on norepinephrine-stimulated mitochondrial uncoupling or maximal respiration was detected in the cultured human adipocytes (Figure 8C,D). Hence, although pharmacological activation of PPARα in primary human adipocytes had a modest stimulatory effect on genes related to browning, these changes did not translate into metabolic changes in uncoupled respiration.

3.7. PPARγ activation but not PPARα activation is able to markedly upregulate cold-induced genes in murine WAT

The *in vivo* and *in vitro* data presented above indicate that PPARα is not required for (cold-induced) adipose tissue browning. This conclusion suggests that a transcription factor other than PPARα may be responsible for the induction of PPAR target genes in inguinal WAT during cold. An obvious candidate is PPARγ, as its expression in inguinal WAT is increased during cold (Figure 9A) [5]. In contrast, expression of PPARδ was very stable in iWAT during cold-induced browning in all available microarray datasets (GSE13432, GSE01080, present study). To explore the possible role of PPARγ, we compared the effect of PPARγ and PPARα activation in mice on the expression of cold-induced genes in adipose tissue using transcriptomics (Figure 9B). In this experiment, wildtype mice were given rosiglitazone or Wy-14,643 in the food for 1 week. Whereas PPARγ activation by rosiglitazone markedly induced the expression of cold-induced genes in WAT, PPARα activation by Wy-14,643 had a minimal effect (Figure 9B). The most highly induced genes by Wy-14,643 in WAT were the PPARα targets *Vnn1* (2.2-fold) and *Fabp1* (3.2-fold), neither of which are induced by cold. These data indicate that PPARγ activation but not PPARα activation is able to markedly upregulate cold-induced genes in murine WAT.

3.8. Chronic cold does not lead to activation of PPARα in the liver

Recently, it was demonstrated that short term cold exposure increases plasma long chain acyl-carnitine levels [43], concomitant with induction of the hepatic expression of several enzymes involved in acylcarnitine metabolism. Since many of these enzymes are under transcriptional control of PPARα, we explored the possibility that PPARα may be important for regulating lipid metabolism in the liver during cold. To that end, we measured the hepatic expression of several genes involved in acylcarnitine metabolism, as well as other target genes of PPARα, in thermoneutral and cold-exposed wildtype and PPARα−/− mice (Figure 10A). While the expression of most genes studied was reduced in the liver of PPARα−/− mice, no

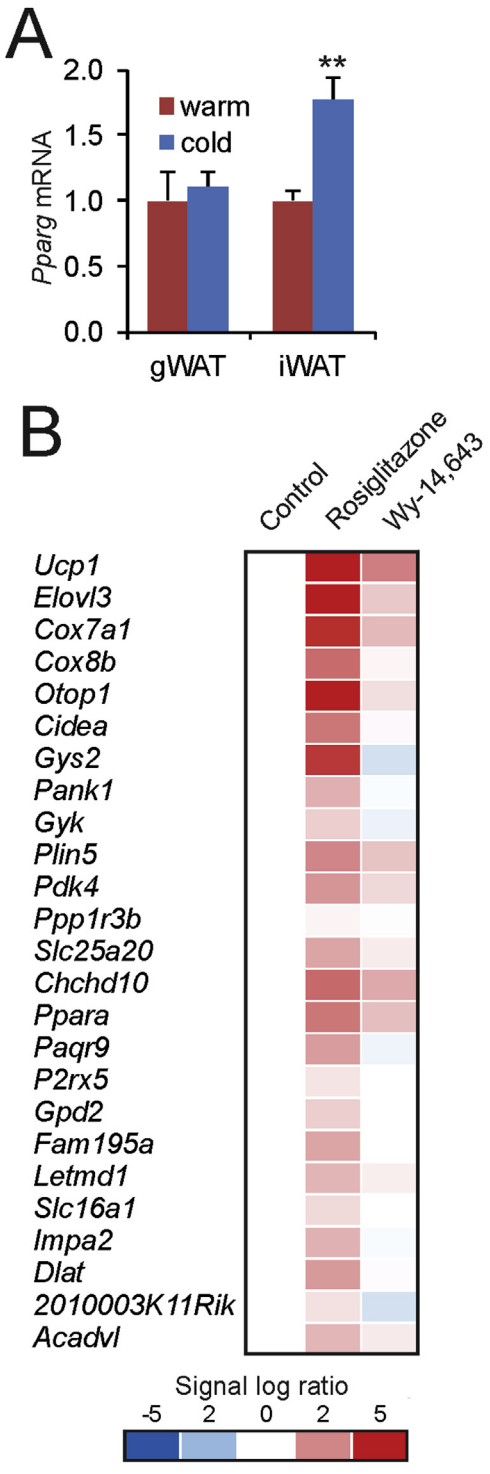

Figure 9: PPARγ activation but not PPARα activation is able to markedly upregulate cold-induced genes in murine WAT. A) Relative gene expression of *Pparg* in gonadal WAT and inguinal WAT of wildtype mice after 10 days at 28 °C (warm, n = 6–8) or 5 °C (cold, n = 10) [51]. Data are presented as mean ± SEM. Asterisk indicates significantly different from thermoneutral mice according to Student's t-test (**P < 0.01). B) Comparative analysis was performed between whole genome expression changes in WAT in response to 10-day cold exposure and in response to 7-day treatment with rosiglitazone (0.01 % wt/wt of feed) or Wy-14,643 (0.1 % wt/wt of feed). The top 25 most highly induced genes by 10-day cold exposure in WAT of wildtype mice were selected. The effect of 1-week treatment with rosiglitazone or Wy-14,643 on the expression of these genes in WAT of wildtype mice is shown (GSE11295). The top 25 list differs from Figure 7, because certain genes were either not present on the microarray used for the rosiglitazone/Wy-14,643 study or did not meet the filtering criteria.

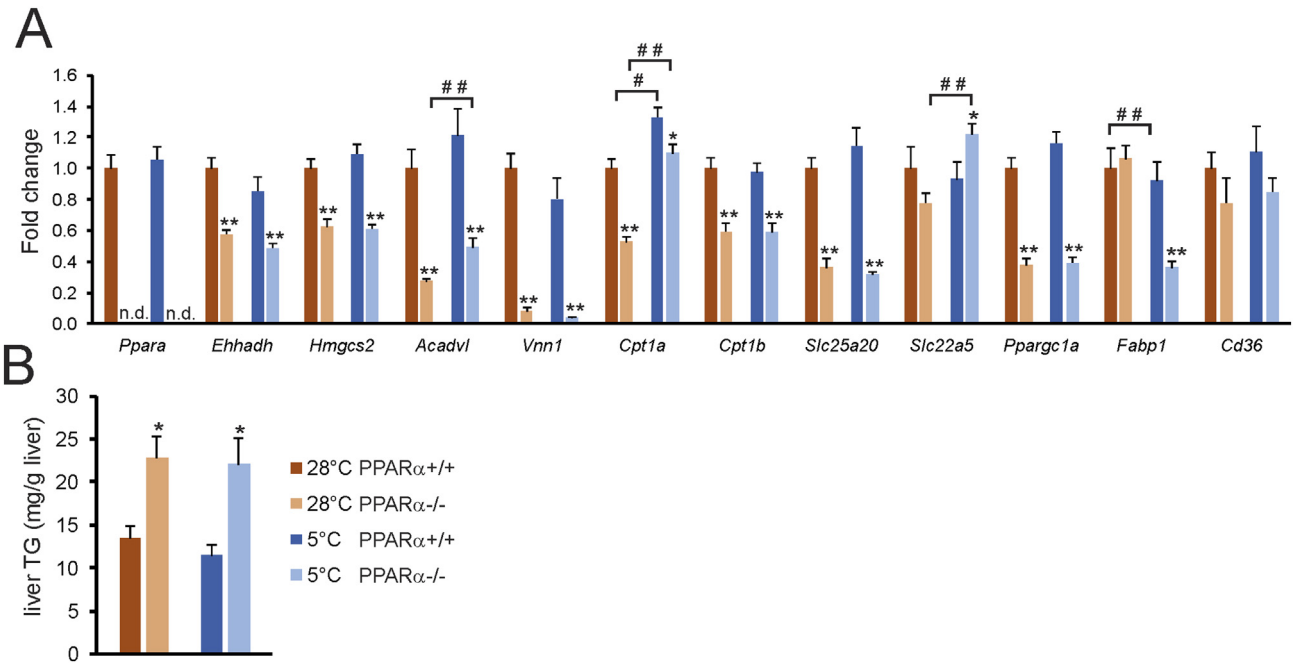

Figure 10: No interaction between cold and PPARα ablation in hepatic gene regulation. (A) Hepatic expression of selected genes in wildtype and PPARα−/− mice exposed to cold (5 °C) or thermoneutrality (28 °C) for 10 days. (B) Liver triglycerides. N = 10 per group. Error bars represent SEM. Asterisk indicates significantly different from wildtype mice under the same conditions according to Student's t-test (*P < 0.05, **P < 0.001). Pound sign indicates significant difference between cold and thermoneutral mice according to Student's t-test (#P < 0.05, ##P < 0.001).

interaction was observed between cold and loss of PPARα, meaning that the effect of loss of PPARα was comparable in cold and thermoneutral conditions (Figure 10A). An exception was *Fabp1*, expression of which was lower in PPARα−/− mice compared to wildtype mice at 5 °C but not at 28 °C. Importantly, the expression of genes involved in acylcarnitine metabolism and of other PPARα targets was refractory to cold. In line with the gene expression data, liver triglyceride levels were higher in the PPARα−/− mice compared to wildtype mice, yet levels were similar in the cold and thermoneutral conditions (Figure 10B). To assess the potential role of PPARα in liver during acute cold, we measured the hepatic expression of the same set of genes in wildtype and PPARα−/− mice exposed to cold for 24 h. Although acute cold caused the marked upregulation of *Cpt1a* and *Slc22a5*, both of which are involved in acylcarnitine metabolism, the induction was similar in wildtype and PPARα−/− mice (Supplemental Figure 2). Other PPARα targets were only weakly activated or not activated at all by acute cold. Together, these data indicate that the role of PPARα in liver does not become more important during acute or chronic cold, suggesting that cold does not lead to activation of PPARα in the liver, unlike during fasting.

4. DISCUSSION

Little is known about the regulatory mechanisms driving the metabolic adaptations during cold-induced browning. Whereas previous studies have found that loss of PPARα leads to attenuation of CL316,243-induced adipose tissue browning [27,29], here we find that PPARα, despite its marked upregulation in inguinal WAT by cold, is completely dispensable for cold-induced browning in mice. Histological analysis of inguinal WAT showed clear browning upon cold but did not reveal any morphological differences between wildtype and PPARα−/− mice. Transcriptomics analysis showed that the cold-induced changes in gene expression in inguinal WAT were fully maintained in the absence of PPARα at the whole genome level, the pathway level, and the level of individual genes. Indeed, cold-sensitive thermogenic genes such as *Ucp1* and *Elovl3* and numerous others were similarly induced by cold in wildtype and PPARα−/− mice. Overall, our data indicate that PPARα is not required for cold-induced browning in inguinal WAT. The lack of effect of PPARα ablation on gene expression in inguinal WAT during cold contrasts starkly with the dramatic effect of PPARα ablation on gene expression in liver during fasting, a well-known PPARα-driven phenomenon.

Several studies have examined the role of PPARα in *in vivo* adipose tissue browning, either by treating mice with synthetic PPARα agonists or by using PPARα−/− mice, yielding somewhat conflicting results. For example, whereas in one study, chronic treatment of mice with the PPARα agonist fenofibrate led to the induction of thermogenic genes and the appearance of multilocular adipocytes in WAT [44], in another study, chronic treatment with fenofibrate failed to cause an increase in multilocular adipocytes in WAT [24]. Treatment of wildtype mice with CL316,243 upregulated PPARα mRNA in white adipose tissue by 10-fold, suggesting a potential role of PPARα in CL316,243-induced browning. Interestingly, CL316,243 triggered morphological changes characteristic of browning in WAT of wildtype but not PPARα−/− mice [29]. Transcriptomics analysis showed that the time-dependent expression changes in WAT following CL316,243 treatment were attenuated in PPARα−/− mice [29]. In agreement with the known role of PPARα in regulating fatty acid catabolism, many of the affected genes were involved in the transport/activation and oxidation of fatty acids. In another study, induction of thermogenic genes such as *Ucp1*, *Elovl3*, and *Cpt1*b by CL316,243 was shown to be attenuated in the absence of PPARα−/−, both at room temperature and at thermoneutrality [27]. These data suggest that PPARα has a stimulatory role in CL316,243-induced adipose tissue browning.

By contrast, our data indicate that PPARα is not required for cold-induced browning. It thus appears that the role of PPARα may be different between CL316,243-induced browning and cold-induced browning. The reason for this difference is not clear but may be related to the more diverse effects of cold versus the more targeted mechanism of action of CL316,243. Alternatively, the possible compensatory role of PPARγ (see below) may be more readily recruitable during cold-induced browning than during CL316,243-induced browning.

Previously, it was shown that PPARα and PPARγ can regulate partially overlapping gene sets [45]. Based on our data, it is not possible to distinguish between the possibility that in wildtype mice: 1) PPARα is not at all involved in gene regulation in inguinal WAT during cold, or 2) PPARα drives the expression of several cold-induced genes in inguinal WAT, yet PPARγ takes over the role of PPARα in PPARα−/− mice. The second scenario is reminiscent of the ability of PPARγ to compensate for the absence of PPARα in livers of PPARα−/− mice chronically fed a high fat diet [46]. In that situation, the expression of PPARγ goes up dramatically [46]. In favor of the first possibility, transcriptomics did not reveal a compensatory increase in PPARγ expression in inguinal WAT of PPARα−/− mice. Moreover, in contrast to PPARγ activation, PPARα activation had only minimal effects on thermogenic gene expression in WAT of wildtype mice. Accordingly, activation of PPARγ but not PPARα likely is a major driver of cold-induced changes in gene expression in inguinal white adipocytes. Even though several cold-induced genes involved in fatty acid catabolism are primarily known as targets of PPARα, it has been shown that under certain conditions, PPARγ is capable of upregulating classical PPARα targets [46,47]. Why PPARα is dramatically upregulated in inguinal WAT during cold if it is not involved in regulating gene expression, remains unclear. The dispensable role of PPARα in cold-induced browning is consistent with the recent finding that PPARα is not required for *in vivo* brown fat function [48].

In contrast to *Ppara* and *Pparg*, the expression of *Ppard* in inguinal WAT is completely refractory to cold. Although the lack of change in *Ppard* expression does not rule out a role of PPARδ in cold-induced browning, it does make it unlikely. Arguing against a role of PPARδ in adipose tissue browning, PPARδ was recently shown to be dispensable for brown fat function [48].

Our experiments and studies of others in primary human adipocytes showed that PPARα activation leads to increased expression of brown fat markers such as *UCP1*, *CIDEA*, *ELOVL3*, and *CPT1B* [27]. Furthermore, when analyzed by transcriptomics, PPARα and PPARγ activation in primary human adipocytes caused the induction of largely overlapping gene sets, reflecting a browning of human white adipocytes [27]. To what extent these changes upon pharmacological PPARα activation reflect a physiological role of PPARα in *in vitro* browning remains unclear. Unfortunately, technical limitations preclude investigation of the influence of inactivation of PPARα on *in vitro* features of browning in primary human adipocytes.

In our study, 10 days of cold exposure caused a large increase in food intake, while it did not change the bodyweight of the mice, underlining the profound increase in energy demand during cold exposure in mice. The huge increase in energy expenditure and thermogenesis allowed the mice to maintain a stable body temperature during the entire 10-day intervention. Importantly, no differences in body temperature were observed between the two genotypes, except for the first 12 h of cold acclimation, during which the PPARα−/− mice had a slightly lower body temperature. The more significant drop in body temperature in the PPARα−/− mice during the first hours of cold exposure is likely caused by the semi-fasting of the mice in the light cycle, when the mice are sleeping. Indeed, fasting by itself has been shown to provoke hypothermia in whole body and liver-specific PPARα−/− mice [15,49]. Based on these considerations, the previously observed decline in body temperature in PPARα−/− mice upon 3 h of cold exposure is probably due to the fact that the mice were fasted at the same time and might not reflect a role of PPARα in cold-induced thermogenesis per se [50].

Recently, it was shown that short term cold exposure leads to elevation of plasma long chain acyl-carnitine levels, concomitant with induction of the expression of enzymes involved in acylcarnitine metabolism in the liver, including *Cpt1b*, *Slc22a5*, *Slc25a20*, and *Crat* [43]. A mechanism was proposed in which NEFA derived from adipose tissue lipolysis activate the nuclear receptor HNF4α in the liver, leading to induction of genes involved in acyl-carnitine production. Since the above genes are all direct targets of PPARα, which is activated by fatty acids, it can be hypothesized that apart from HNF4α, PPARα may also be involved in the stimulation of acyl-carnitine synthesis during short term cold. In our study, however, we could not find any evidence for upregulation of genes involved in carnitine synthesis after chronic cold. In addition, other target genes of PPARα were also not induced in the liver after chronic cold. Interestingly, hepatic expression of *Cpt1a* and *Slc22a5*, both of which are involved in acylcarnitine metabolism, was elevated by acute cold. However, this induction was independent of PPARα. Overall, these data suggest that hepatic PPARα is not activated by acute or chronic cold. Intriguingly, hepatic expression of *Fabp1* was lower in PPARα−/− mice specifically at 5 °C, which may account for the elevated NEFA levels in PPARα−/− mice during cold.

In conclusion, we find that cold-induced changes in gene expression in inguinal WAT are unaltered in mice lacking PPARα, indicating that PPARα is dispensable for cold-induced browning.

ACKNOWLEDGEMENTS

This research was supported by CVON ENERGISE grant CVON2014-02.

CONFLICT OF INTEREST

None declared.

APPENDIX A. SUPPLEMENTARY DATA

Supplementary data related to this article can be found at https://doi.org/10.1016/j.molmet.2018.01.023.

REFERENCES

[1] Peschechera, A., Eckel, J., 2013. "Browning" of adipose tissue—regulation and therapeutic perspectives. Archives of Physiology and Biochemistry 119: 151—160.

[2] Cousin, B., Cinti, S., Morroni, M., Raimbault, S., Ricquier, D., Penicaud, L., et al., 1992. Occurrence of brown adipocytes in rat white adipose tissue: molecular and morphological characterization. Journal of Cell Science 103(Pt 4):931—942.

[3] Christian, M., 2015. Transcriptional fingerprinting of "browning" white fat identifies NRG4 as a novel adipokine. Adipocyte 4:50—54.

[4] Sidossis, L.S., Porter, C., Saraf, M.K., Borsheim, E., Radhakrishnan, R.S., Chao, T., et al., 2015. Browning of subcutaneous white adipose tissue in humans after severe adrenergic stress. Cell Metabolism 22:219—227.

[5] Seale, P., 2015. Transcriptional regulatory circuits controlling Brown fat development and activation. Diabetes 64:2369—2375.

[6] Gross, B., Pawlak, M., Lefebvre, P., Staels, B., 2016. PPARs in obesity-induced T2DM, dyslipidaemia and NAFLD. Nature Reviews Endocrinology.
[7] Tateno, C., Yamamoto, T., Utoh, R., Yamasaki, C., Ishida, Y., Myoken, Y., et al., 2015. Chimeric mice with hepatocyte-humanized liver as an appropriate model to study human peroxisome proliferator-activated receptor-alpha. Toxicologic Pathology 43:233–248.
[8] Varga, T., Czimmerer, Z., Nagy, L., 2011. PPARs are a unique set of fatty acid regulated transcription factors controlling both lipid metabolism and inflammation. Biochimica et Biophysica Acta 1812:1007–1022.
[9] Gearing, K.L., Gottlicher, M., Teboul, M., Widmark, E., Gustafsson, J.A., 1993. Interaction of the peroxisome-proliferator-activated receptor and retinoid X receptor. Proceeding of the National Academy of Science of the USA 90: 1440–1444.
[10] Issemann, I., Prince, R.A., Tugwood, J.D., Green, S., 1993. The retinoid X receptor enhances the function of the peroxisome proliferator activated receptor. Biochimie 75:251–256.
[11] Keller, H., Dreyer, C., Medin, J., Mahfoudi, A., Ozato, K., Wahli, W., 1993. Fatty acids and retinoids control lipid metabolism through activation of peroxisome proliferator-activated receptor-retinoid X receptor heterodimers. Proceeding of the National Academy of Science of the USA 90:2160–2164.
[12] Georgiadi, A., Kersten, S., 2012. Mechanisms of gene regulation by Fatty acids. Advances in nutrition 3:127–134.
[13] Bookout, A.L., Jeong, Y., Downes, M., Yu, R.T., Evans, R.M., Mangelsdorf, D.J., 2006. Anatomical profiling of nuclear receptor expression reveals a hierarchical transcriptional network. Cell 126:789–799.
[14] Escher, P., Braissant, O., Basu-Modak, S., Michalik, L., Wahli, W., Desvergne, B., 2001. Rat PPARs: quantitative analysis in adult rat tissues and regulation in fasting and refeeding. Endocrinology 142:4195–4202.
[15] Kersten, S., Seydoux, J., Peters, J.M., Gonzalez, F.J., Desvergne, B., Wahli, W., 1999. Peroxisome proliferator-activated receptor alpha mediates the adaptive response to fasting. Journal of Clinical Investigation 103: 1489–1498.
[16] Leone, T.C., Weinheimer, C.J., Kelly, D.P., 1999. A critical role for the peroxisome proliferator-activated receptor alpha (PPARalpha) in the cellular fasting response: the PPARalpha-null mouse as a model of fatty acid oxidation disorders. Proceeding of the National Academy of Science of the USA 96: 7473–7478.
[17] Regnier, M., Polizzi, A., Lippi, Y., Fouche, E., Michel, G., Lukowicz, C., et al., 2017. Insights into the role of hepatocyte PPARalpha activity in response to fasting. Molecular and Cellular Endocrinology.
[18] Kersten, S., 2014. Integrated physiology and systems biology of PPARalpha. Molecular Metabolism 3:354–371.
[19] Lehmann, J.M., Moore, L.B., Smith-Oliver, T.A., Wilkison, W.O., Willson, T.M., Kliewer, S.A., 1995. An antidiabetic thiazolidinedione is a high affinity ligand for peroxisome proliferator-activated receptor gamma (PPAR gamma). Journal of Biological Chemistry 270:12953–12956.
[20] Tontonoz, P., Hu, E., Spiegelman, B.M., 1994. Stimulation of adipogenesis in fibroblasts by PPAR gamma 2, a lipid-activated transcription factor. Cell 79: 1147–1156.
[21] Barak, Y., Nelson, M.C., Ong, E.S., Jones, Y.Z., Ruiz-Lozano, P., Chien, K.R., et al., 1999. PPAR gamma is required for placental, cardiac, and adipose tissue development. Molecular Cell 4:585–595.
[22] Majithia, A.R., Tsuda, B., Agostini, M., Gnanapradeepan, K., Rice, R., Peloso, G., et al., 2016. Prospective functional classification of all possible missense variants in PPARG. Nature Genetics 48:1570–1575.
[23] Fukui, Y., Masui, S., Osada, S., Umesono, K., Motojima, K., 2000. A new thiazolidinedione, NC-2100, which is a weak PPAR-gamma activator, exhibits potent antidiabetic effects and induces uncoupling protein 1 in white adipose tissue of KKAy obese mice. Diabetes 49:759–767.
[24] Koh, Y.J., Park, B.H., Park, J.H., Han, J., Lee, I.K., Park, J.W., et al., 2009. Activation of PPAR gamma induces profound multilocularization of adipocytes in adult mouse white adipose tissues. Experimental & Molecular Medicine 41: 880–895.
[25] Petrovic, N., Walden, T.B., Shabalina, I.G., Timmons, J.A., Cannon, B., Nedergaard, J., 2010. Chronic peroxisome proliferator-activated receptor gamma (PPARgamma) activation of epididymally derived white adipocyte cultures reveals a population of thermogenically competent, UCP1-containing adipocytes molecularly distinct from classic brown adipocytes. Journal of Biological Chemistry 285:7153–7164.
[26] Gray, S.L., Dalla Nora, E., Backlund, E.C., Manieri, M., Virtue, S., Noland, R.C., et al., 2006. Decreased brown adipocyte recruitment and thermogenic capacity in mice with impaired peroxisome proliferator-activated receptor (P465L PPARgamma) function. Endocrinology 147:5708–5714.
[27] Barquissau, V., Beuzelin, D., Pisani, D.F., Beranger, G.E., Mairal, A., Montagner, A., et al., 2016. White-to-brite conversion in human adipocytes promotes metabolic reprogramming towards fatty acid anabolic and catabolic pathways. Molecular Metabolism 5:352–365.
[28] Digby, J.E., Montague, C.T., Sewter, C.P., Sanders, L., Wilkison, W.O., O'Rahilly, S., et al., 1998. Thiazolidinedione exposure increases the expression of uncoupling protein 1 in cultured human preadipocytes. Diabetes 47: 138–141.
[29] Li, P., Zhu, Z., Lu, Y., Granneman, J.G., 2005. Metabolic and cellular plasticity in white adipose tissue II: role of peroxisome proliferator-activated receptor-alpha. American Journal of Physiology, Endocrinology and Metabolism 289: E617–E626.
[30] Xue, B., Coulter, A., Rim, J.S., Koza, R.A., Kozak, L.P., 2005. Transcriptional synergy and the regulation of Ucp1 during brown adipocyte induction in white fat depots. Molecular and Cellular Biology 25:8311–8322.
[31] Jankovic, A., Golic, I., Markelic, M., Stancic, A., Otasevic, V., Buzadzic, B., et al., 2015. Two key temporally distinguishable molecular and cellular components of white adipose tissue browning during cold acclimation. Journal of Physiology 593:3267–3280.
[32] Bolstad, B.M., Irizarry, R.A., Astrand, M., Speed, T.P., 2003. A comparison of normalization methods for high density oligonucleotide array data based on variance and bias. Bioinformatics 19:185–193.
[33] Irizarry, R.A., Bolstad, B.M., Collin, F., Cope, L.M., Hobbs, B., Speed, T.P., 2003. Summaries of Affymetrix GeneChip probe level data. Nucleic Acids Research 31:e15.
[34] Dai, M., Wang, P., Boyd, A.D., Kostov, G., Athey, B., Jones, E.G., et al., 2005. Evolving gene/transcript definitions significantly alter the interpretation of GeneChip data. Nucleic Acids Research 33:e175.
[35] Sartor, M.A., Tomlinson, C.R., Wesselkamper, S.C., Sivaganesan, S., Leikauf, G.D., Medvedovic, M., 2006. Intensity-based hierarchical Bayes method improves testing for differentially expressed genes in microarray experiments. BMC Bioinformatics 7:538.
[36] Subramanian, A., Tamayo, P., Mootha, V.K., Mukherjee, S., Ebert, B.L., Gillette, M.A., et al., 2005. Gene set enrichment analysis: a knowledge-based approach for interpreting genome-wide expression profiles. Proceeding of the National Academy of Science of the USA 102:15545–15550.
[37] Sanderson, L.M., Degenhardt, T., Koppen, A., Kalkhoven, E., Desvergne, B., Muller, M., et al., 2009. Peroxisome proliferator-activated receptor b/d (PPARb/d) but not PPARa serves as a plasma free fatty acid sensor in liver. Molecular and Cellular Biology 29:6257.
[38] Stienstra, R., Duval, C., Keshtkar, S., van der Laak, J., Kersten, S., Muller, M., 2008. Peroxisome proliferator-activated receptor gamma activation promotes infiltration of alternatively activated macrophages into adipose tissue. Journal of Biological Chemistry 283:22620–22627.
[39] Alex, S., Lange, K., Amolo, T., Grinstead, J.S., Haakonsson, A.K., Szalowska, E., et al., 2013. Short-chain fatty acids stimulate angiopoietin-like 4 synthesis in human colon adenocarcinoma cells by activating peroxisome proliferator-activated receptor gamma. Molecular and Cellular Biology 33: 1303–1316.

[40] Broeders, E.P., Nascimento, E.B., Havekes, B., Brans, B., Roumans, K.H., Tailleux, A., et al., 2015. The bile acid chenodeoxycholic acid increases human brown adipose tissue activity. Cell Metabolism 22:418—426.

[41] Rosell, M., Kaforou, M., Frontini, A., Okolo, A., Chan, Y.W., Nikolopoulou, E., et al., 2014. Brown and white adipose tissues: intrinsic differences in gene expression and response to cold exposure in mice. American Journal of Physiology, Endocrinology and Metabolism 306:E945—E964.

[42] Xue, Y., Petrovic, N., Cao, R., Larsson, O., Lim, S., Chen, S., et al., 2009. Hypoxia-independent angiogenesis in adipose tissues during cold acclimation. Cell Metabolism 9:99—109.

[43] Simcox, J., Geoghegan, G., Maschek, J.A., Bensard, C.L., Pasquali, M., Miao, R., et al., 2017. Global analysis of plasma lipids identifies liver-derived acylcarnitines as a fuel source for brown fat thermogenesis. Cell Metabolism 26, 509—522 e506.

[44] Rachid, T.L., Penna-de-Carvalho, A., Bringhenti, I., Aguila, M.B., Mandarim-de-Lacerda, C.A., Souza-Mello, V., 2015. Fenofibrate (PPARalpha agonist) induces beige cell formation in subcutaneous white adipose tissue from diet-induced male obese mice. Molecular and Cellular Endocrinology 402:86—94.

[45] Hummasti, S., Tontonoz, P., 2006. The peroxisome proliferator-activated receptor N-terminal domain controls isotype-selective gene expression and adipogenesis. Molecular Endocrinology 20:1261—1275.

[46] Patsouris, D., Reddy, J.K., Muller, M., Kersten, S., 2006. Peroxisome proliferator-activated receptor alpha mediates the effects of high-fat diet on hepatic gene expression. Endocrinology 147:1508—1516.

[47] Yu, S., Matsusue, K., Kashireddy, P., Cao, W.Q., Yeldandi, V., Yeldandi, A.V., et al., 2003. Adipocyte-specific gene expression and adipogenic steatosis in the mouse liver due to peroxisome proliferator-activated receptor gamma1 (PPARgamma1) overexpression. Journal of Biological Chemistry 278:498—505.

[48] Lasar, D., Rosenwald, M., Kiehlmann, E., Balaz, M., Tall, B., Opitz, L., et al., 2018. Peroxisome proliferator activated receptor gamma controls mature brown adipocyte inducibility through glycerol kinase. Cell Reports 16:760—773.

[49] Montagner, A., Polizzi, A., Fouche, E., Ducheix, S., Lippi, Y., Lasserre, F., et al., 2016. Liver PPARalpha is crucial for whole-body fatty acid homeostasis and is protective against NAFLD. Gut 65:1202—1214.

[50] Ahmadian, M., Abbott, M.J., Tang, T., Hudak, C.S., Kim, Y., Bruss, M., et al., 2011. Desnutrin/ATGL is regulated by AMPK and is required for a brown adipose phenotype. Cell Metabolism 13:739—748.

[51] Dijk, W., Heine, M., Vergnes, L., Boon, M.R., Schaart, G., Hesselink, M.K., et al., 2015. ANGPTL4 mediates shuttling of lipid fuel to brown adipose tissue during sustained cold exposure. eLife 4.

